Spatial pattern of sea surface temperature and chlorophyll-a trends in relation to hydrodynamic processes in the Alborán Sea

Benyounes ABDELLAOUI[1], Federico FALCINI[2], Tarik BAIBAI[1], Karim HILMI[1,3], Omar ETTAHIRI[1], Rosalia SANTOLERI[2], Rachida HOUSSA[1], Hassan NHHALA[4], Hassan ER-RAIOUI[4] and Laila OUKHATTAR[5]

[1] National Institute for Fisheries Research, Oceanography Department, Morocco

[2] Istituto di Scienze Marine - Consiglio Nazionale delle Ricerche, Roma, Italy

[3] Intergovernmental Oceanographic Commission of UNESCO (IOC/UNESCO)

[4] University of Abdelmalek Saidi, LEORN, Faculty of Sciences, Tangier, Morocco

[5] University of Cadi Ayad, Ecole supérieure de technologies, Essaouira, Morocco

Corresponding author: Benyounes ABDELLAOUI; byounes2011@gmail.com

Contributing Editor: Sarantis SOFIANOS

Abstract

Environmental conditions such as temperature, planktonic biomass, and ocean currents play an important role in the development and distribution of marine species. This work aims to estimate, in a high spatial resolution, the actual trends of sea surface temperature (SST) and chlorophyll-a concentration (Chl-a) and to assess the relationship with the local hydrodynamic conditions in the Alborán Sea. To investigate these objectives, time series of SST and Chl-a of satellite sensor data were analyzed during 20 years from January 2001 to December 2020, using the Seasonal-Trend-Loess (STL) decomposition method and the Mann-Kendall seasonality test. The results, obtained with a 95% of confidence, showed that the Alborán Sea basin is subject to sea surface warming evaluated at 0.027 ± 0.008 ° C per year, related to the warming of the Atlantic water mass, which contributes to a decrease of productivity evaluated at -0.0024 ± 0.0003 µg /l per year of Chl-a concentration. These trends are not homogeneous over the entire basin area but show a large regional variation between different parts of the Alborán Sea due to the hydrodynamic process of the Atlantic Jet - Western Alboran Gyre system (AJ-WAG), which is more active especially in summer/autumn seasons and contribute largely to these changes by mixing the waters of the Atlantic Ocean and the Mediterranean Sea.

Keywords: Alborán Sea; SST; Chlorophyll-a (Chl-a); Time series; trends; STL; Mann-Kendall; Western Alboran Gyre (WAG); Atlantic Jet (AJ).

Introduction

Climate change is expected to affect oceanic conditions with increases in sea surface temperature (SST) as well as changes in water-mass proprieties and hydrodynamic conditions (IPCC, 2007). Estimating the long-term of these modifications is crucial for evaluating the current state of the oceans and assessing the impact on marine productivity and fishery yields (Allain *et al.*, 2001; Lafuente *et al.*, 2005; Lett *et al.*, 2007; Sabatés *et al.*, 2007; Santos *et al.*, 2007; Rykaczewski *et al.*, 2008; Palatella *et al.*, 2014; Xu *et al.*, 2015; Falcini *et al.*, 2015; Vargas-Yáñez *et al.*, 2020). For example, a change in water temperature may negatively impact the spawning and the feeding of larval survival (Miller *et al.*, 1992, Moyle *et al.*, 2004). Abdellaoui *et al.* (2017) showed that higher temperatures combined with low productivity could lead to a gradual decline in pelagic fish yields over the sub-

sequent years. According to Vargas-Yáñez *et al.* (2020), who studied the inter-annual variability of sardine abundance, this abundance was strongly related to the wind intensity and chlorophyll-a (Chl-a) concentration during the previous year.

It is, therefore, important to understand the spatial and temporal patterns of water-mass properties in the natural environment to assess the sustainable development of marine species and their exploitation (Allain *et al.*, 2001; Lafuente *et al.*, 2005; Lett *et al.*, 2007). Recently, many multidisciplinary studies have attempted to define diagnostic tools to link the potential impact of climate change on marine resources to all the data of biological, physical, and biogeochemical oceanographic measurements, using statistical and numerical models (Tugores *et al.*, 2011; Palatella *et al.*, 2014; Hammond *et al.*, 2020). Sea surface temperature (SST) and Chlorophyll-a concentration (Chl-a), a proxy of marine phytoplankton biomass,

136

Mediterr. Mar. Sci., 25/1, 2024, 136-150

are the most important parameters to be evaluated. Both control growth of marine species and are also very easily measured using remote sensing at high spatial resolution (Santoreli *et al.*, 1994; Colella *et al.*, 2016; Pisano *et al.*, 2020).

The Mediterranean Sea has been identified as a climate change hot-spot by the scientific community (Giorgi, 2006). This sea is a semi-enclosed basin with only one connection to the open Atlantic Ocean via the Strait of Gibraltar (14 km width, 300 m depth). The Strait of Sicily divides it into the Eastern and Western Mediterranean. Numerous studies have shown that the Mediterranean Sea has undergone rapid warming in recent decades: Rixen *et al.* (2005) found that the average temperature of the upper layer of the Western Mediterranean Sea (between 0-150 m) has increased between the years 1980 and 2000. In the same way, Criado-Aldeanueva *et al.* (2008) found that the SST of the Mediterranean Sea has increased by 0.06 °C per year during 1992-2005. More recently, Pastor *et al.* (2019) have shown that the seawater warming in the Mediterranean Sea is not uniform over the entire basin, but there are two regions with warming intensities evolving differently. The central Mediterranean, as well as parts of the Algerian and Moroccan coasts have a weak warming trend; the Levantine-Aegean basin shows a higher warming trend (Nykjaer, 2009; Skliris *et al.*, 2012; Shaltout & Omstedt, 2014). The same observation has been made by Pisano *et al.* (2020), estimating the trends of 0.036 ± 0.006 °C per year for the western part of the Mediterranean basin and 0.048 ± 0.006 °C per year for the eastern part, the Levantine-Aegean Sea, using a satellite-based dataset from the Copernicus Marine Environment Monitoring Service (CMEMS).

As previously mentioned, Chl-a concentration is a significant variable. It is a direct indicator of phytoplankton biomass (Sabatés *et al.*, 2007; Santos *et al.*, 2007) and is widely used to understand the evolution of the functioning of marine ecosystems (Rykaczewski *et al.*, 2008; Xu *et al.*, 2015; Falcini *et al.*, 2015; Colella *et al.*, 2016). According to several studies, the concentration of Chl-a in the Mediterranean Sea basin decreases from west to east, and a clear separation between the two sub-basins can be shown in the Strait of Sicily (Volpe *et al.*, 2012; Colella *et al.*, 2016). High concentrations of Chl-a have been observed in coastal areas, particularly near river mouths, that provide significant continental nutrient loads (Colella *et al.*, 2016). Using satellite observation data and a Bayesian spatiotemporal model, Hammond *et al.* (2020) showed that regional Chl-a trends are significantly different from zero for 18 of the 23 regions and vary within a range of ±1.8% per year. It is typically more positive at mid to high latitudes. The uncertainty follows a different pattern, appearing to be partially dependent on the ocean region, high in the North Atlantic and low in the Southern Ocean. The global average shows a net positive trend of 0.08 ± 0.35% per year, which highlights the importance of considering changes in Chl-a concentration at the regional level (Hammond *et al.*, 2020).

The Alborán Sea is a part of the Mediterranean basin, located near the Strait of Gibraltar between the European Spanish coast in the north and the Moroccan African coast in the south. The hydrodynamic processes here are controlled by a mesoscale structure of 100–150 km in diameter, called the Western Anticyclone Gyre or Western Alboran Gyre (WAG) and the Atlantic Jet (AJ), which are the main factors of the exchange of water mass balance between the Mediterranean basin and the Atlantic Ocean across the Strait of Gibraltar. The flowing mass of Atlantic water feeds the Western Alboran Gyre by a meandering hydrodynamic structure, and it sometimes allows the formation of the second anticyclone gyre in the eastern part, called the Eastern Alboran Gyre (EAG) (Fig. 1).

This AJ-WAG-EAG system is the main engine that rules water mass distribution in the Alborán Sea. It is regulated by the interaction of several hydro-metrological processes at both local and regional levels (atmospheric forcing). The drivers of the WAG's rotation may include wind stress, lateral forcing from the AJ, and the
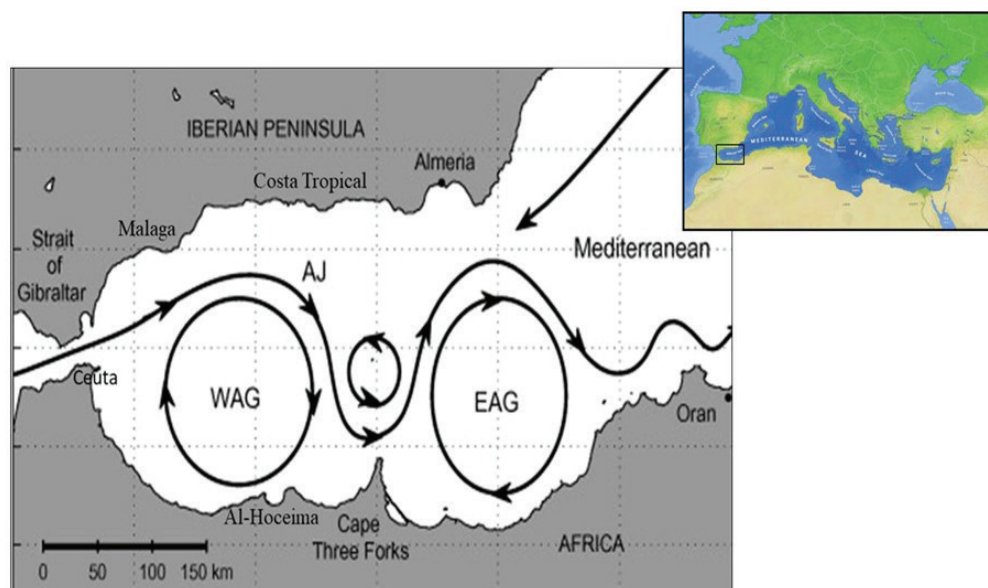

Fig. 1: Location of the Alborán Sea: black box on map of the Mediterranean Sea (source Wikipedia) and its main hydrodynamic system: AJ, WAG, and EAG (after Sánchez-Garrido *et al.*, 2013).

Mediterr. Mar. Sci., 25/1, 2024, 136-150

137

added anticyclonic vorticity from the rising deep waters as they approach the Strait of Gibraltar (Bryden & Stommel, 1982). Atmospheric pressure-driven flows are also shown to have the potential to destabilize the circulation by dramatically rising the potential velocity flux within a time scale of some days (Sánchez-Garrido *et al.*, 2013).

The present work aims to evaluate the trends of SST and Chl-a concentration at the regional level in the Alborán Sea. The main objective is to highlight the current trends and patterns of these variables and to discuss the factors that affect their variability in relationship to the hydrodynamic processes of the WAG as the main structure controlling the water and material flows between different parts of the basin. Understanding these factors may help to understand the impact of climate change on the productivity and sea warming in the Alborán Sea and in all Mediterranean basin during the last two decades (Criado-Aldeanueva & Soto-Navarro, 2020; Vargas-Yáñez *et al.*, 2010; MedECC, 2020). The impact of warming on the gyre marine systems, as is the case for the Alborán Sea, is not well known and no literature discusses this relationship in the Mediterranean Sea.

Materials and Methods

Datasets

Satellite sensors can provide information on changes in physical and biological parameters of Ocean and sea surface waters by estimating their trends and understanding global changes. A long time series of more than 20 years of monthly data from January 2001 to December 2020 of SST and Chl-a concentrations were obtained by processing different satellite data available on marine scientific platforms.

Monthly sea surface temperature was obtained by processing satellite data from the MODIS / Aqua imaging radiometer sensor at 4-km spatial resolution, available on the NASA Ocean Color Web server (https://oceancolor.gsfc.nasa.gov).

The chlorophyll-a concentrations data time series was downloaded from the OCEANCOLOUR_MED_BGC_L4_MY / CMEMES dataset at 1-km resolution produced by the Italian National Research Council (CNR, Rome, Italy), obtained by means of the Mediterranean Ocean Color regional algorithms MedOC4 (Volpe *et al.*, 2019) and AD4 (Berthon & Zibordi, 2004).

We have not used the NASA Ocean Color Web server because several authors have shown that the algorithm (OC3M) proposed for MODIS generally overestimates the chlorophyll-a concentration in the Mediterranean Sea (D'Ortenzio *et al.*, 2002). This problem is even enhanced when the algorithm is used for the Alborán Sea (Gómez-Jakobsen *et al.*, 2016).

The monthly time series available in NETCDF raster format were extracted over the study area, i.e., Alborán Sea, and merged as ASCII format to two different grids square matrix: 4 km resolution for SST and 1 km for Chl-a data. Each matrix pixel presents monthly times series values of SST and Chl-a concentrations from 2001 to 2020.

Due to the errors of terrestrial interference in the radiometric signal of satellite images, the pixels closest to the coast (4 – 8 km from the coastline, depending on the bathymetry) were excluded from the processing series.

Methodological approach

For an appropriate assessment of the SST and Chl-a concentration trends, the time series were analyzed based on the method of decomposition of the signal into seasonal and annual components (trends without the effects of the seasons). The magnitude of positive or negative trends of each time series are validated by the Mann-Kendall (MK), which is a nonparametric estimation method (Wernand *et al.*, 2013; Fu *et al.*, 2016; Colella *et al.*, 2016; Abdellaoui *et al.*, 2017; Pisano *et al.*, 2020; Moradi, 2020). This method is based on the computation of statistical test parameter (S) and its variance Var (S) defined as follows (Mann, 1945; Kendall, 1948):

$$S = \sum_{i=1}^{n-1} \sum_{j=i+1}^{n} sgn(x_j - x_i)$$

$$sgn(x_j - x_i) = \begin{cases} -1 \ if \ (x_j - x_i) > 0 \\ 0 \ if \ (x_j - x_i) = 0 \\ 1 \ if \ (x_j - x_i) < 0 \end{cases}$$

$$Var(S) = \frac{1}{18}[n(n-1)(2n+5) - \sum_{p=1}^{q} t_p(t_p - 1)(2t_p + 5)]$$

where
(x_i, x_j) are the values of the time series (with $j = i +1$);
n is the number of data;
q is the number of related groups (a related group is a set of data samples with the same value);
t_p is the number of data points in the p-th group.

The parameter Sen's slope (β), expressing the magnitude of the trend, is estimated by the following formula (Sen, 1968):

$$\beta = Median \left(\frac{x_j - x_i}{j - i} \right), \qquad j > i$$

The (S) parameter, the variance (Var) (S), and the magnitude (β) of both SST and Chl-a time series are estimated from monthly data for the period between 2001 and 2021, after applying the Seasonal-Trend-Loess (STL) (Cleveland *et al.*, 1990; Perretti, 2015). The STL method consists of transforming the main series (X_t) into different fundamental components:

$$X_t = Z_t + S_t + \dot{\varepsilon}_t \qquad 1 \leq t \leq n$$

- A regular and periodic seasonal component (S_t) which represents the seasonal fluctuations of the time series (X_t);
- A residual component, which represents the noise (t) with irregular fluctuations, generally a weak intensity but of random frequency of the time series (X_t).
- A global component (Z_t) which represents the net

138

Mediterr. Mar. Sci., 25/1, 2024, 136-150

global trend of the time series (X_t) without the seasonal influence and residual fluctuation;

The decomposition analysis is based on the smoothing values of the periodic windows of 12 months for global trends and six months for seasonal trends. The values of the global component (without the effect of seasons) estimated by the STL method are used to define the parameter Sen's slope. The statistical Mann-Kendall test is used to quantify the significance of the trends in order to accept or refute results depending on the p-value of a 95% confidence interval. To better highlight the results, the trend is also expressed by using the relative changes (i.e., % yr^{-1}) obtained by dividing (β) by the climatological value for the entire period (January 2001 – December 2020).

The seasonal trends are estimating by applying the Mann-Kendall test and the Sen's slope method for each seasonal (winter, spring, summer, autumn) time series.

Statistical analyses using the linear model (LM) and the Additive General Model (GAM) were used to fit the correlation between the SST trends and Atlantic Multidecadal Oscillation (AMO) index values download from http://www.psl.noaa.gov/data/timeseries/AMO/

Results

Climatological Data Analysis

Figure 2 presents the evolution of the monthly averages of SST and Chl-a concentration data in the Alborán Sea between January 2001 and December 2020. A clear biannual cycle can be seen for both parameters, expressed by two significant seasonal phases. A linear trend applied to the means annuals data shows a very weak magnitude of the slopes, but is still positive for SST and negative for Chl-a.

Monthly mean values of the Chl-a concentration are highly dispersed; the standard deviation is ~ 0.33 for an average of 0.27 µg /l displaying a very strong coefficient variation of 1.22. The seasonal variations of SST, as for the Chl-a, are randomly dispersed. In contrast, annual mean variations are rather stable around an average of 18.72 °C, displaying a low standard deviation of 2.90 and a small coefficient variation of 0.15.

Generally, SST and Chl-a follow seasonal fluctuations. Both exhibit a two-phase cycle: the first one from October to April, characterized by a relatively low temperature with a minimum observed in February and by a maximum production of chlorophyll-a in March. The second phase occurs between May and October, and is characterized by a higher temperature with the maximum in August and by the lowest Chl-a concentration of the year (Fig. 2).

Figure 3 presents the spatial distribution of mean climatological data of SST and Chl-a concentration. We can easily recognize the spatial pattern of the Alborán Sea AJ-WAG-EAG structure as a very important hydrodynamic process of ventilation and material transfer. The permanent penetration of Atlantic waters under the action of the Atlantic Jet (AJ), through the Strait of Gibraltar, leads to permanent mixing of the water column down to 300 m deep. These spatial and vertical variations lead to the formation of very clearly distinguished hydrological regions in terms of temperature and nutrient richness:

The northwestern part, located at the entrance of the Strait of Gibraltar between Ceuta and Malaga, shows a colder temperature (17–18.5 °C) and relatively high concentration of chlorophyll-a (>1 µg / l). Unlike other areas, the Chl-a concentration in this basin area is higher. A strong phytoplankton activity is recognized throughout the year, especially from the spring to summer seasons (Sarhan *et al.,* 2000). It is considered an upwelling area with high productivity, which takes place more evident-
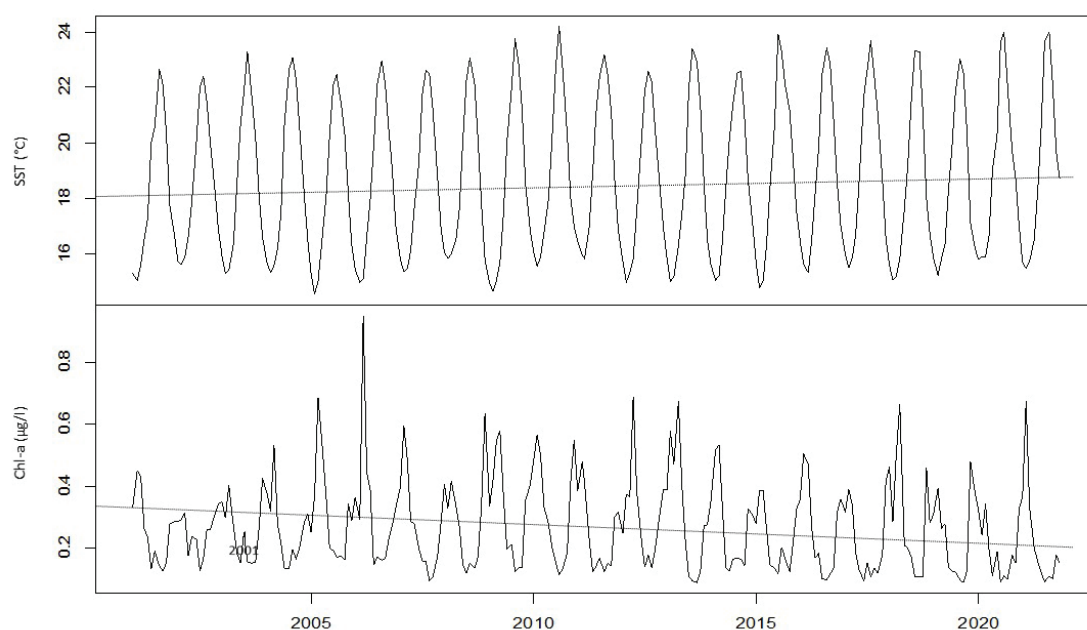

Fig. 2*:* Evolution of monthly mean of SST (upper panel) and the Chl-*a* (lower panel) of the Alborán Sea between January 2001 and December 2020. Solid lines represent the averages of the monthly means data for all pixels. Dashed lines represent the linear slope.
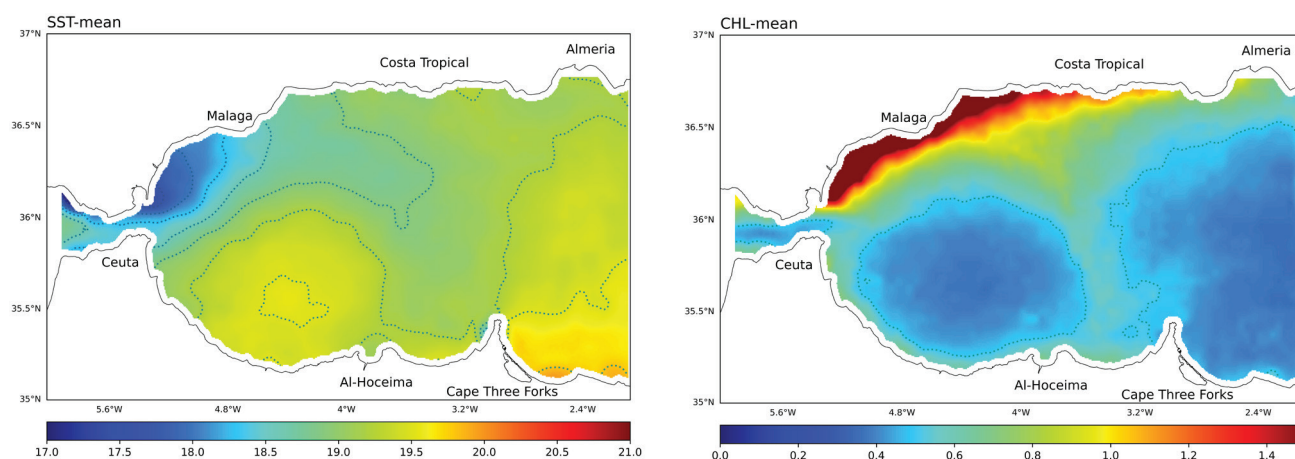
Fig. 3*:* Spatial distribution of annual climatological mean of SST (left panel) and Chl-a concentration (right panel) (monthly data of the Alborán Sea between January 2001 and December 2020).

ly from March to June (Fig. 4) when the phytoplankton activity is high and thermal contrast is stronger, easily observed in satellite images (Fig. 3).

The north central part of the Alborán basin, where the Atlantic flow moves toward the south (WAG), allows the ventilation of colder Atlantic waters (18 – 19 °C) rich in plankton. The Chl-a concentrations vary between 0.5 and 1 µg / l. The Al-Hoceima area located at the south of the Alborán basin at the eastern part of Cape Three Forks (Moroccan coast) has the same characteristics as the Spanish coast, in particular the Costa Tropical area (see Fig. 3). This connection is well marked during the hot season due to the absence of the destabilizing factors of the AJ-WAG system, especially meteorological forcing occurring during the winter in the Atlantic Ocean, which leads to the formation of sub-flow water and large tidal waves at the entrance of the Strait of Gibraltar (Shaltout *et al.*, 2014, Wirasatriya *et al.*, 2020). However, from May to December, this gradient is broken, and the whole space is evolving in the AJ-WAG system dynamic, which takes over the atmospheric processes and makes the variability of SST and Chl-a concentration in the Alborán Sea

very pronounced.

In the southern part of the basin, the gradual southward shift of the Atlantic water mass (AJ), due to Coriolis force especially in the dry season and with the easterly wind (summer and autumn), generates two gyres from each side of Cape Three Forks (Morocco) (Fig. 3). In the western side, water is evolving in an anticyclonic movement, forming the WAG characterized by a moderate temperature (19–22 °C) and lower Chl-a concentration (< 0.5 ug /l). On the eastern side (SE), the Atlantic water, initially represented by the Atlantic Jet moving south, deviates northwesterly and forms a clear thermal front in contact with the Mediterranean water mass, which sometimes is involved in an anticyclonic movement called Eastern Alboran Gyre (EAG). These waters are warmer with temperatures varying between 19 and 24 C° with lower Chl-a concentrations (< 0.5 µg /l).

Trend analysis

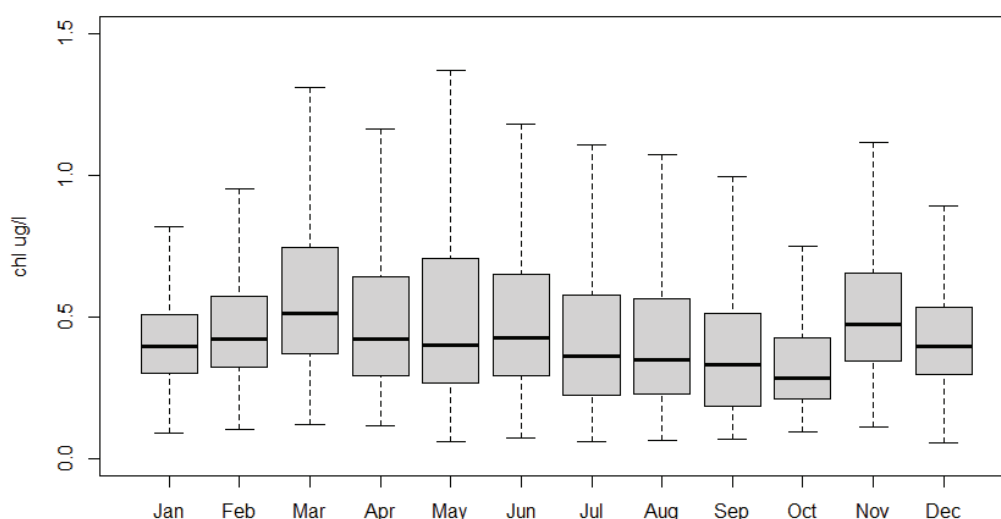For a proper assessment of SST and Chl-a concentra-

Fig. 4*:* Monthly means of Chl-*a*, from January 2001- December 2020 in the northwestern part of the Alborán Sea (coastal area of Malaga).

tion trends in the Alborán Sea, the monthly time series of the two parameters were analyzed by decomposition of the signal data into seasonal and global components based on the STL method. This method transforms the main series (observed data) into different fundamental components, namely a global component (trend), a seasonal component, and a residual component representing noise with irregular fluctuations. Figure 5 represents the results of this decomposition based on data from January 2001 to December 2021.

SST trends: the time series of the global component (SST trend) presented in Figure 5 shows a very weak upward positive linear trend. The estimation of the magnitude of this slope, based on monthly data for the entire period (2001 – 2020) using the Sen's slope parameter for all the basin, shows that the Alborán Sea is subject to an increase of sea surface temperature evaluated at 0.027 ± 0.008 °C / year (p-value = 0.000001). This warming is apparently not uniform across all the basin, but shows high spatial variability. The S-slope varies between 0.039

and 0.014°C / year (Table 1).

The northwestern part, as an important upwelling area especially the coastal area, appears to be more affected by this warming, recording the strongest annual trend of ~ 0.39 °C per year, which represent 0.25 % yr[1] of the climatological SST value. Several other areas are also affected, in particular the south central and the north eastern parts, perfectly reproducing the same spatial pattern of the water mass dynamics of the AJ-WAG system, showing the implication of the hydrodynamic processes in the context of this warming at the regional level (Fig. 1 and Fig. 6). The eastern part (eastern Cape Three Forks) and the western area near the strait of Gibraltar recorded lower trend warming (< 0.1% yr[1]) during recent years (Fig. 6). These areas constitute the cores of the gyres with a permanent mixing water of Mediterranean and Atlantic mass, modifying the initial water properties of the Atlantic Jet (AJ) into Modified Atlantic Waters (MAW).

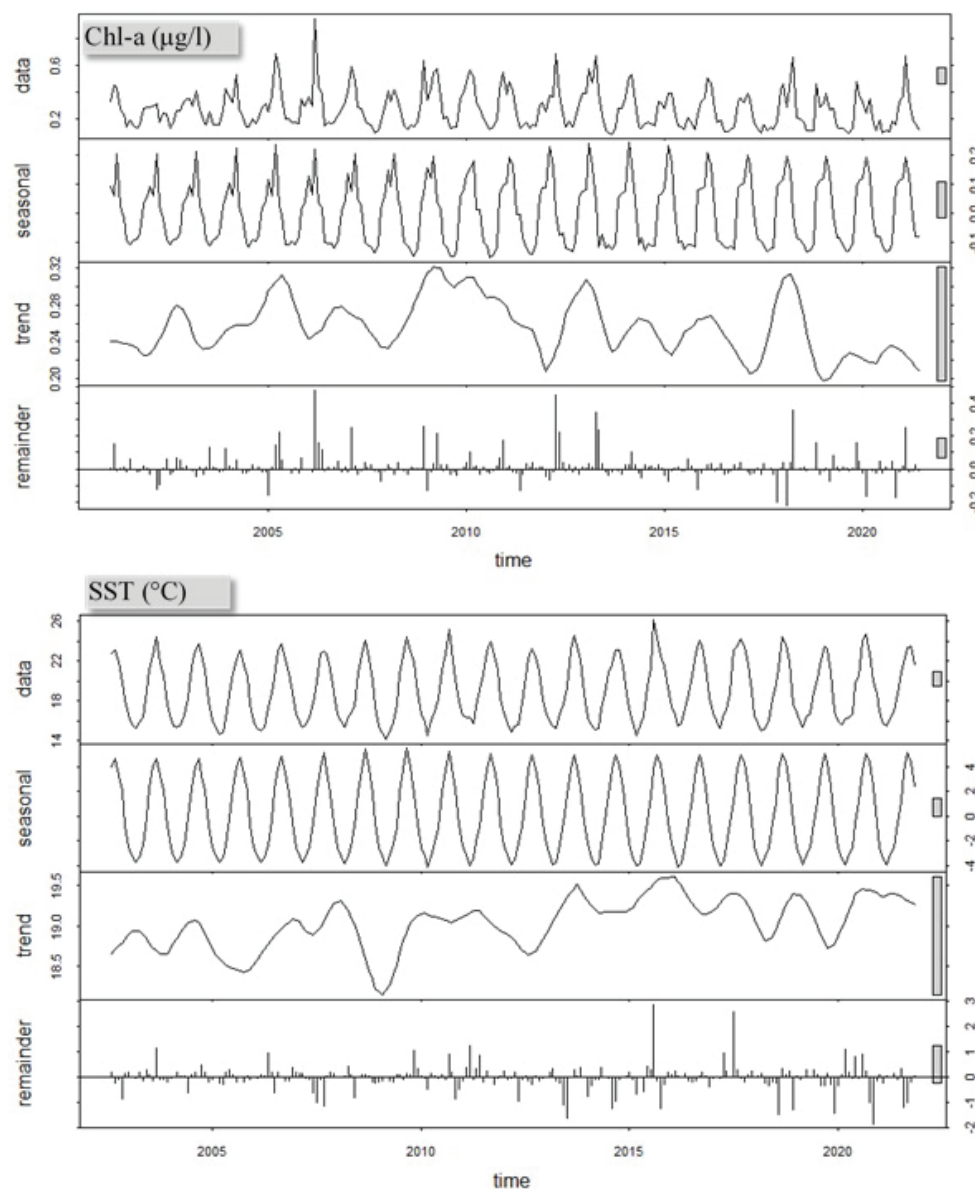On the other hand, the analysis of seasonal trends by applying the Mann-Kendall test and the Sen-slope meth-

Fig. 5: Seasonal and global (trend) evolution of monthly SST (lower panel) and Chl-*a* (upper panel) of the Alborán Sea from January 2001 to December 2020.

Mediterr. Mar. Sci., 25/1, 2024, 136-150

141

Table 1. The SST trend slopes (°C yr⁻¹) and statistical parameters for different areas in the Alborán Sea.

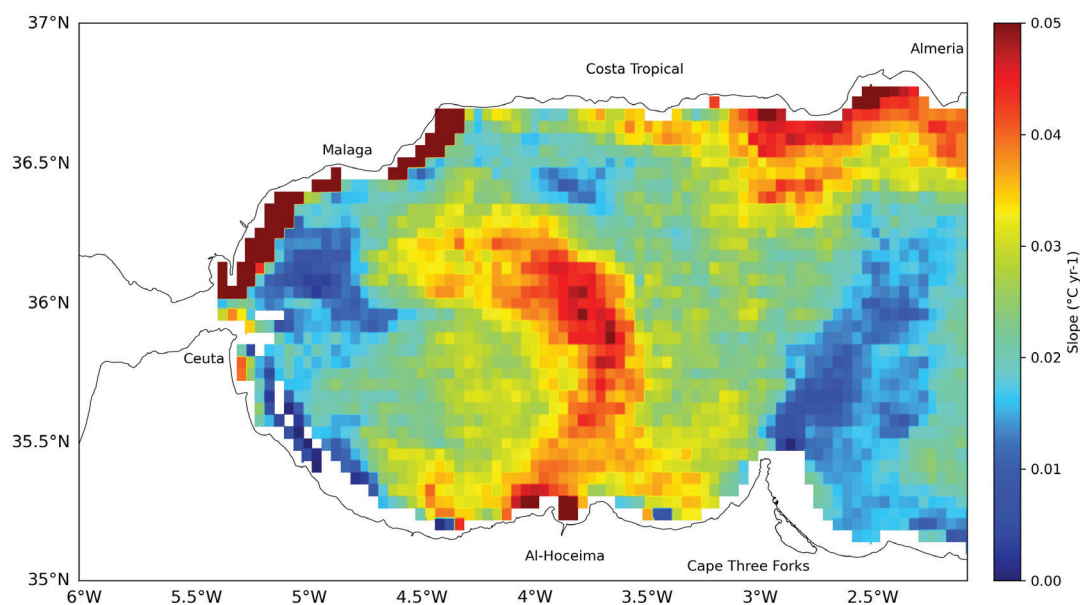|	Global trend	P-value	S-slope (°C yr⁻¹)	% yr⁻¹
NW Alboran	increasing	0.0000	0.039	0.25
NC Alboran	increasing	0.0000	0.029	0.16
NE Alboran	increasing	0.0000	0,031	0.15
SW Alboran	increasing	0.0000	0.019	0,10
SC Alboran	increasing	0.0000	0.032	0.18
SE Alboran	increasing	0.0000	0.014	0.07

Fig. 6: Spatial structure of SST trends in the Alborán Sea (only statistically significant results are presented).

od to estimate the trends for each seasonal time series shows that this warming is mainly linked to the increase of temperature during the summer and autumn seasons. This means that most changes of temperature waters in Alborán Sea happen in these seasons when most of hydrodynamic process are active. Data processing and mapping of the positive and statistically significant SST slope values (P value < 0.05) demonstrate that the strongest trends are recorded in the drifting Atlantic Jet waters to the south and to then to the north, allowing the formation of the two anticyclonic gyres (Fig. 7). The cores of these two structures have non-significant warming trends compared to the relative surrounding areas (Atlantic Jet Water). This may indicate that the Western Alboran Gyre is a dominant feature during this period of summer-autumn and strongly affects spatial variability. The strongest trends are recorded off the Spanish coast, in the northern Alborán Sea (+ 0.1 °C/year) (Fig. 7).

Chl-a trends: opposite to the SST trends, Chl-a concentrations in the Alborán Sea show a highly significant decreasing trend, evaluated at 0.0024 ± 0.0003 µg /l per year (p-value = 2.22e-16) (Table. 2).

The spatial pattern of trends obviously shows the same areas identified in the spatial trends pattern as of the SST previously presented: the coastal upwelling area, the gyre, and the mixing zones (Fig. 8). The values in the coastal upwelling zone (south eastern part of the Iberian Peninsula) and Moroccan south-central part (eastern part of Cape Three Forks) recorded the highest decreasing trend values (> -1 % yr⁻¹).

Regarding the seasonal trends of the Chl-a concentration (winter, spring, summer, and autumn), the results show negative trends in summer and autumn for the most areas of the basin (Fig. 9). The highest values of this decrease follows the spatial structure of the Atlantic Water Jet (AJ). The pattern is strongly linked to the Western Alboran Gyre (WAG) especially in the summer. In the autumn, the areas most affected by this decrease are those located in the southern coastal part of the basin, Al-Hoceima Bay as well as Bettoya Bay located at the eastern part of Cape Three Forks. The winter and spring seasons contribute less to the global decrease of chlorophyll-a in the basin compared to the autumn and the summer seasons. The impact is only clear in certain coastal zones, in particular the Spanish upwelling areas linked to the westerly wind in winter and near the river mouths where the input of nutrients contributes to the development of phytoplankton in the spring season.

Table 2. The Chl-a trend slopes and statistical parameters for different areas in the Alborán Sea.

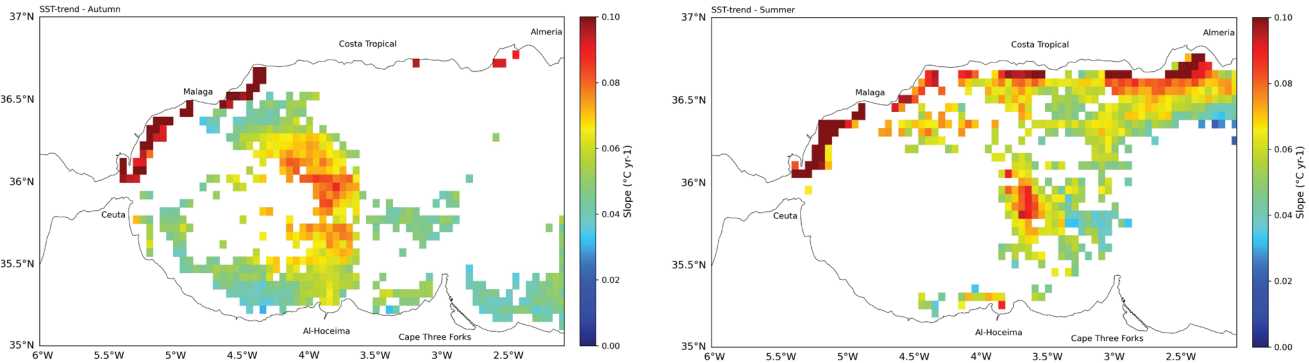|	Global Trend	P-value	S-slope (μg/l yr⁻¹)	% yr⁻¹
NW Alboran	decreasing	0.0000	-0.012	-1.74
NC Alboran	no trend	0.1709	-0.001	-0.24
NE Alboran	decreasing	0.0183	-0.002	-0.47
SW Alboran	decreasing	0.0000	-0.002	-0.71
SC Alboran	decreasing	0.0000	-0.004	-1.25
SE Alboran	decreasing	0.0001	-0.002	-0.83

Fig. 7: Summer (left panel) and autumn (right panel) spatial structures of SST trends in the Alborán Sea (only statistically significant results are presented).
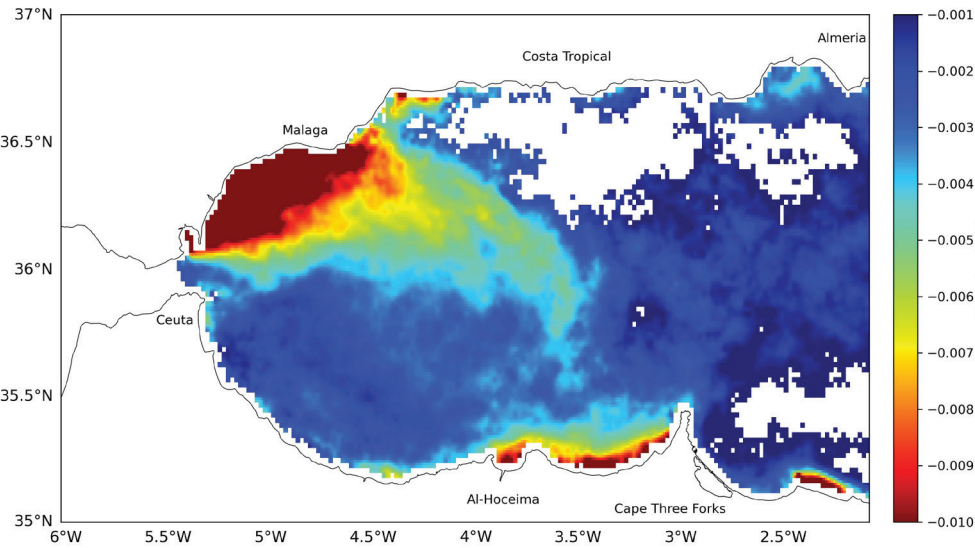

Fig. 8: Spatial structure of Chlorophyll-*a* concentration trends in the Alborán Sea (only statistically significant results are presented).
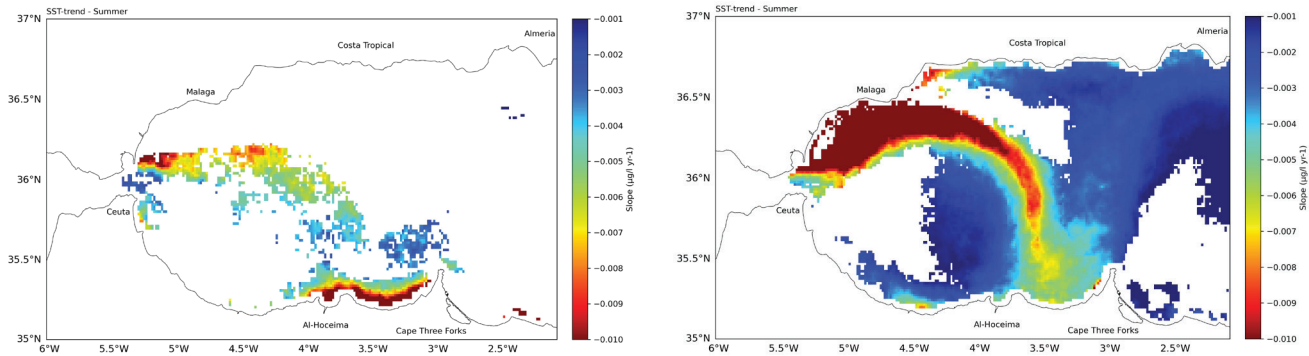

Fig. 9: Summer (Left panel) and autumn (right panel) spatial structures of Chlorophyll-a concentration trends in the Alborán Sea (only statistically significant results are presented).

Discussion

Since the end of the 1970s, the Mediterranean Sea surface water temperature (SST) has been steadily increasing until the end of 2010 (Pastor *et al.*, 2019). According to several authors, this increase is linked to warming air temperatures in the northern hemisphere and the heat absorption by the North Atlantic Ocean (Vargas-Yáñez, 2010; Krauzig *et al.*, 2020). The Alborán Sea, as part of the western Mediterranean Sea, is immediately exposed to all these changes taking place in the Atlantic Ocean since a very strong baroclinic jet of Atlantic water mass is regularly entering the basin through the Strait of Gibraltar.

The present study confirms this seawater warming in the Alborán Sea, which is estimated at 0.027 ± 0.008 °C / year, closer to that found recently by Pisano *et al.* (2020) of 0.036 ± 0.006 °C / year for the western Mediterranean basin. Considering the entire period surveyed (2001-2020), this warming is evaluated at 0.54 °C, equal to what was estimated between 1985 and 2006 by Nykjaer *et al.* (2009) and Vargas-Yáñez *et al.* (2008). This clearly indicates that the increase in surface water temperature in the Alborán Sea is not only confirmed but is still in progress. No slowdown, as described by Macias *et al.* (2013) using the retrospective projection of SST is taking place in the Alborán Sea. The Atlantic Multidecadal Oscillation (AMO) index is always in a positive phase, leading to warming of the Atlantic waters and subsequently of the Alborán Sea (Fig. 10).

Focusing more on the study period between 2001 and 2020 and comparing the evolution of the global components (trend) of SST and AMO, we found that both parameters have the same trend pattern with a positive slope. The minimum warming period observed between 2001 and 2009 corresponds exactly to the minimum amplitude of the AMO index, whilst the warmest period observed between 2009 and 2017 corresponds exactly to the maximum amplitude of the AMO index. The statistical analysis using a linear model (LM) and a nonlinear model as the Additive General Model (GAM) shows that the two parameters are correlated. The r-squared value is 0.43 (p-value $\sim 2 \times 10\text{-}16$), which clearly shows a close relationship between the two parameters (Fig. 11).

To properly evaluate this link at a local scale, we assessed the spatial pattern of the correlation at each pixel by comparing the signal of evolution of AMO with the signal of the local trend in the Alborán Sea. Figure 12 presents the results of this comparison in terms of the correlation coefficient between the SST trend of each pixel and the AMO trend. Results show a general positive correlation between the two signals, in agreement with Pisano *et al.* (2020) and Lopez-Parages *et al.* (2022). The correlation is high in the northern part of study area and in the central part of southern area, where there is a big influence of the West Alboran Gyre off the Moroccan coastal area. No correlation is observed off the Gibraltar Strait, where strong tidal currents and mixing processes may hide the influence of AMO on the SST trend, as well as off the East Alboran Gyre, which is supposed to be more connected to the whole Mediterranean SST pattern rather than just to the AMO signal (Pisano *et al.*, 2020).

This positive correlation between the two signals means that the two systems, the Atlantic Ocean and the Alborán Sea, have the same trend towards a general progressive warming of their sea surface waters which are strongly connected. Obviously, this warming is not uniform within the basin of the Alborán Sea but presents strong spatial variability. The increase in sea surface water temperature mainly affects the upwelling zone (southeastern part of the Iberian Peninsula), the gyre system, and the south-central Moroccan part (eastern part of Cape Three Forks). The spatial configuration of the areas of significant trends is quite the same as that of the eastward drifting Atlantic water mass, gradually modified along its path through the basin, particularly in summer and autumn. The AJ-WAG system stands out as the most important hydrodynamic and biogeochemical process of this trend variability, especially in the summer and in autumn period, by controlling the water mass exchanges between the Mediterranean and the Atlantic Ocean and the vertical mixing processes of the columns of water
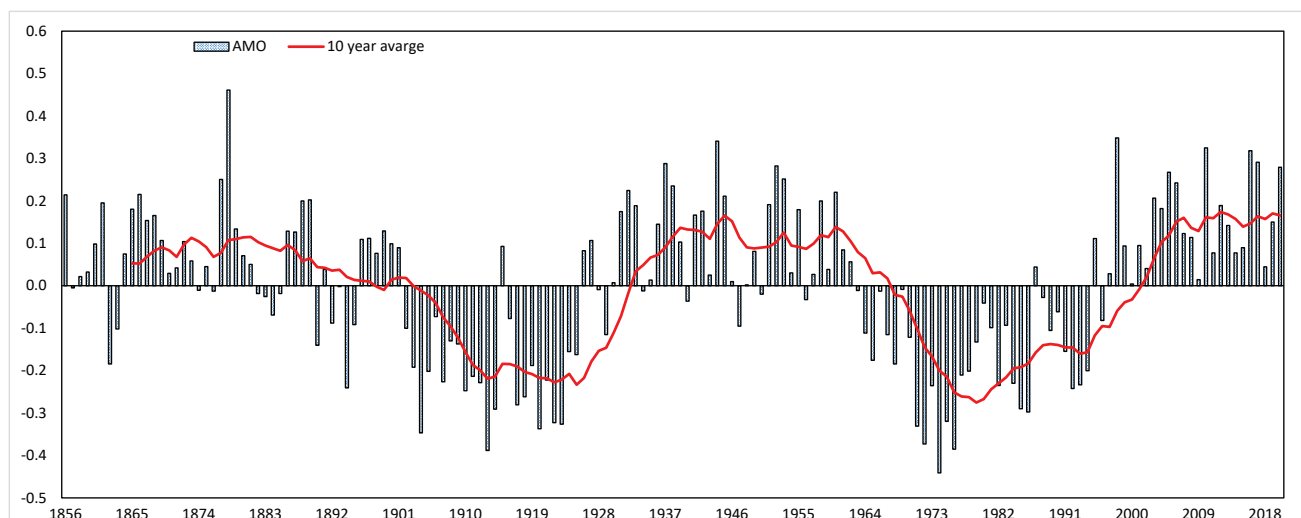

Fig. 10: Atlantic Multidecadal Oscillation (AMO) index values from 1856 to 2020 (data source http://www.psl.noaa.gov/data/timeseries/AMO/
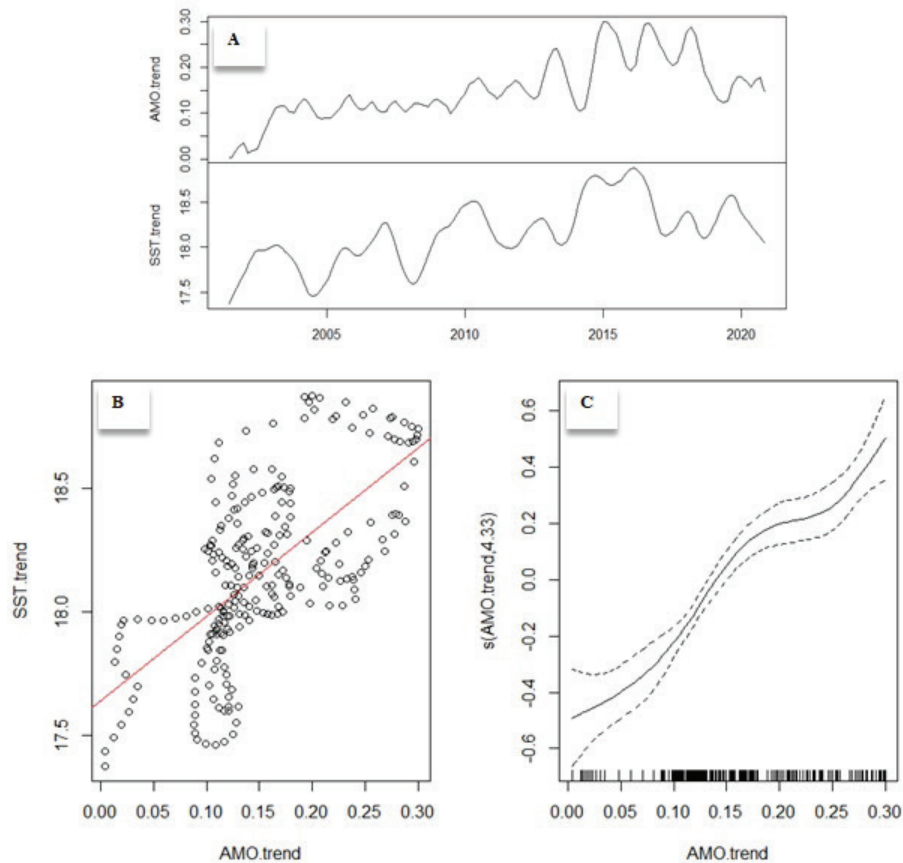
Fig. 11: Relationship between the global component (trend) of SST and AMO index between January 2001 to December 2020 as monthly evolution (**A**); linear relationship LM (**B**), and smoothing nonlinear relationship GAM (**C**).
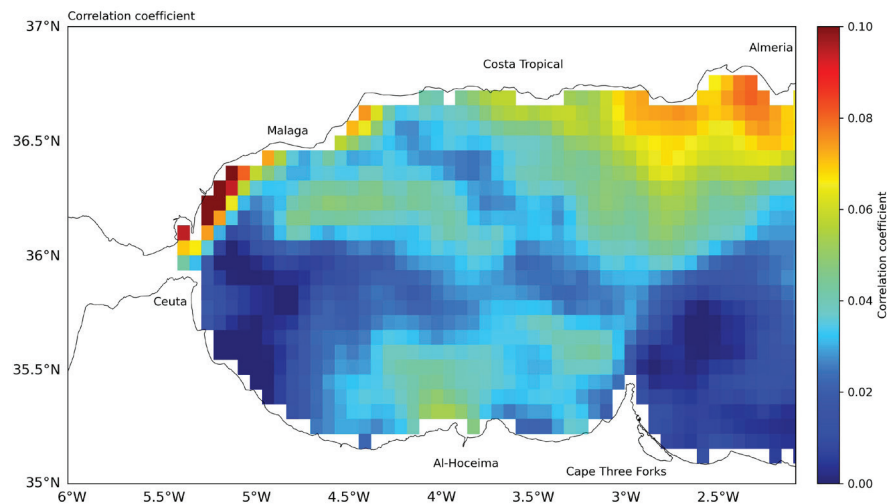

Fig. 12: Spatial correlation between SST trends and AMO trends between January 2001 and December 2020.

(Siokou-Frangou *et al.*, 2010).

Besides this warming of the basin, the Alborán Sea is also subject to a decline of Chl-a concentrations, estimated at -0.0024 ± 0.0003 µg /l per year. The northwest part appears to be the most affected area, with more than -0.012 µg /l per year, equal to -1.7% per year of the Chl-a climatological value (equating a loss of 0.24 µg/l during the last 20 years). The most negative trends were observed in the northwestern part of the Alborán Sea and were found in summer, strongly linked to the WAG. In the autumn, the areas most affected by the decrease of

Chl-a are those located in the southern coastal part of the Alborán Sea: Al-Hoceima Bay, as well as the Bettoya Bay located at eastern part of Cape Three Forks, which recorded the highest increase of sea surface temperature estimated at 0.032 °C per year and a decrease of chlorophyll-a concentration evaluated at -0.004 µg/l per year equal to -1.25% y^{-1} of climatological value. The same results were shown by several authors in different areas in the Mediterranean Sea, by using satellite time series data to estimate the trends of chlorophyll-a concertation. Gómez-Jakobsen *et al.* (2022) estimated a negative trend

Mediterr. Mar. Sci., 25/1, 2024, 136-150

145

on the Spanish coast. The chlorophyll-a concentration reduced in a single decade from 10% (1% y^{-1}) in coastal waters to 20% (2% y^{-1}) in offshore waters. In the same way, by applying the Mann-Kendall test and the Sens's method for trend estimation to the Chl-a concentration de-seasonalized satellite monthly time series as obtained from the X-11 technique, Colella *et al.* (2016), showed a rather complex pattern of both negative and positive Chl-a trends. The coastal region affected by the Rhone River plume (i.e., the Gulf of Lion) shows a wide negative trend (~ 5% yr^{-1}). A similar pattern was observed in the northwest Aegean Sea (i.e., Thermaikos Gulf), which is also characterized by a negative trend of ~ 7% yr^{-1}. A positive trend was detected along the Costa Blanca (south-east of the Spanish coast), in the Ligurian–Provençal basin, as well as in the gyre area of Rhodes. These three regions show trend values of ~ 7% yr^{-1}, ~ 6% yr^{-1}, and ~ 5% yr^{-1}, respectively.

As an oligotrophic basin, Chl-a concentration in the Mediterranean Sea is dominated by winter-spring bloom (D'Ortenzio & D'Alcalà, 2009); it is controlled by vertical mixing (Siokou-Frangou *et al.*, 2010) and in a specific region, it is mainly associated to upwelling phenomena (Garcia-Gorriz & Carr, 2001). A decrease in Chl-a concertation indicates an alteration of hydrodynamic and biogeochemical conditions that are allowing the development of phytoplankton biomass. According to Sarhan *et al.* (2000), the development of Chl-a in this area is controlled by two mechanisms: the southward drifting of the Atlantic Jet water (AJ) and westerly winds, which allow the formation of Ekman transport. This last process which occurs mainly in winter, contributes strongly to the fertilization of the area, while the other, even if it contributes less compared to Ekman transport process, occurs in the dry season when the contribution of rivers is almost low. Recent studies have shown that the viability of upwelling in this area is strongly related to the variability of climatic oscillations of the North Atlantic Ocean (González-Lan-

chas *et al.*, 2020). In the Alborán Sea, winds blow mostly from the west during winter and shift to easterly during summer.

By analyzing wind data from the period 1980 – 2000, no significant change was detected in the wind regime, especially near the upwelling areas (Fig. 13). The same characteristics in terms of direction and speed were observed, if we ignore, however, a slight increase in the high speed percentage of the easterly winds in the last 20 years. Winds are mainly zonal in the Alborán Sea (Fig. 13). Easterlies and westerlies blow with the same strength and are similarly likely except for slight seasonal variations. The strongest winds in either direction east or west occur during the winter, whereas the mildest winds are found during the summer. In the summer, easterlies are also somewhat more frequent than westerlies.

The overall zonal orientation of the Alborán Sea shoreline makes it suitable for wind-driven coastal upwelling specially on the north coast of the basin where more recurrent and stronger upwelling occur along the Spanish coast by the west winds. The analysis of wind speed seasonal anomalies over the period 2000 – 2020 does not show any significant trend in the wind field (both for easterlies and westerlies) that could be associated with a change in Chl-a or SST anomalies in the upwelling areas (Fig. 14). Indeed, as the westerly wind has not experienced significant change on particular in winter and spring season in the last years (Fig.14), we believe that reduction of chlorophyll-a in this area is related to water mass warming of the sea surface layer affecting the vertical mixing and metabolic responses of phytoplankton communities than the decrease of the efficiency of the wind-induced mixing (Mercado *et al.*, 2012; Behrenfeld *et al.*, 2016; Mercado *et al.*, 2022; Vargas-Yañez *et al.*, 2022; Lopez-Parages *et al.*, 2022). The analysis of the correlation coefficients between monthly/seasonal SST and Chl-a anomalies during this period as a spatial pixel-by-pixel correlation show that most areas of the
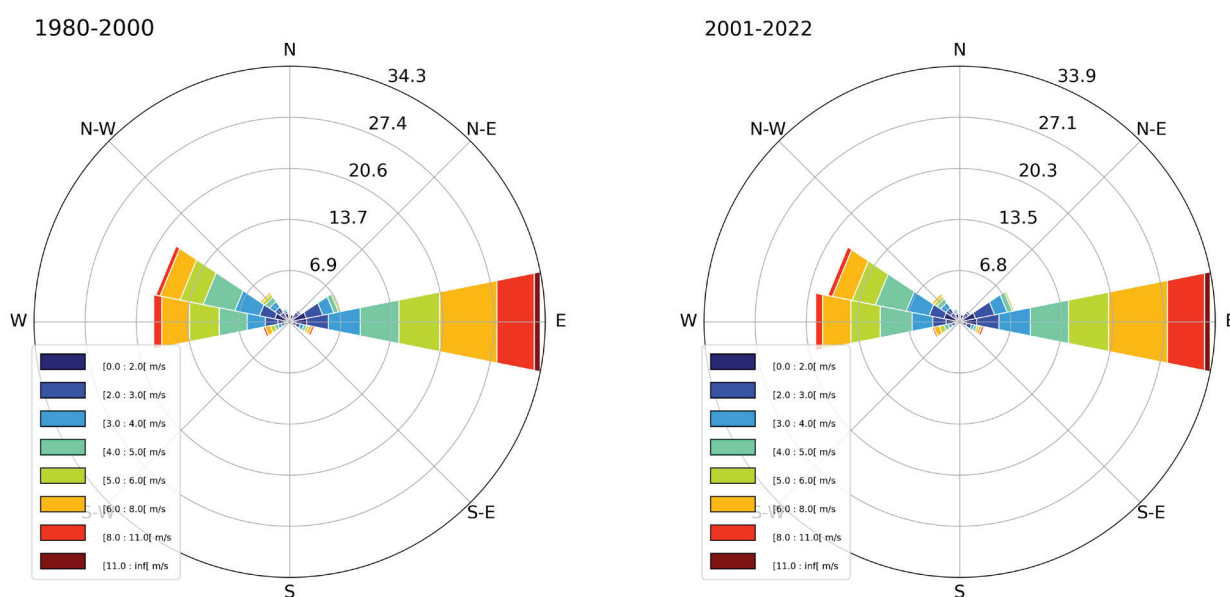

Fig. 13: Distribution of wind speed and direction from 1980 to 2000 (left panel) and from 2001 to 2022 (right panel). Source data MERRA-2.
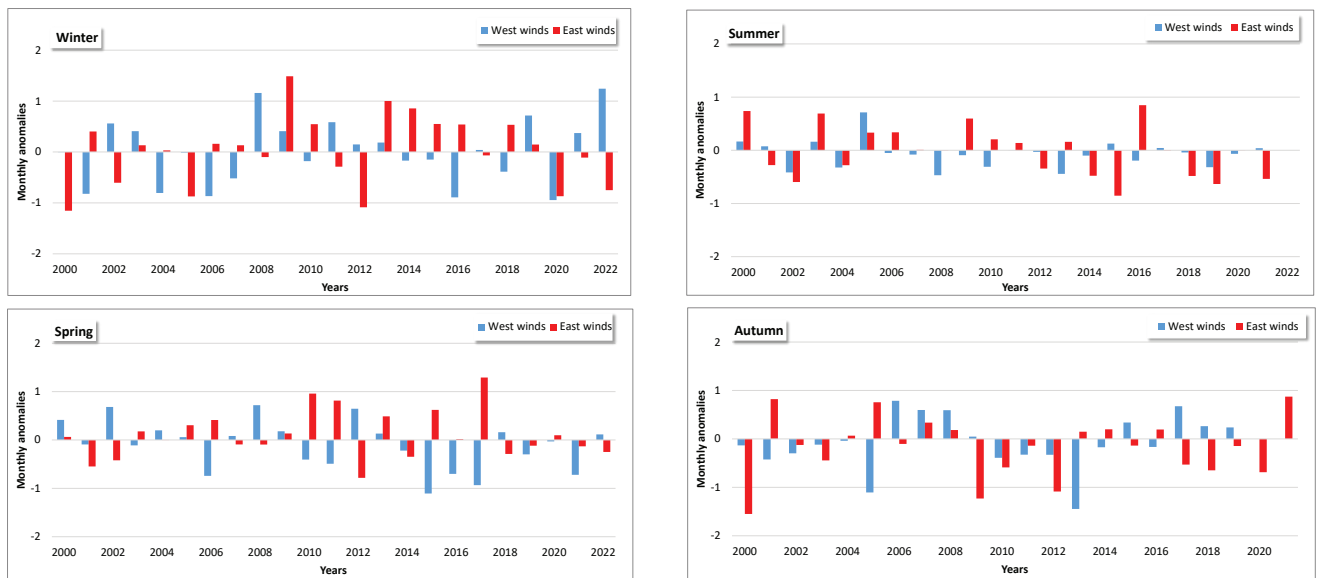
Fig. 14: Evolution of monthly anomalies of wind speed data over the Alborán Sea between 2000 to 2022. Data source: MERRA-2.

Table 3. Correlation coefficients between monthly/seasonal SST and Chl-a anomalies for different areas in the Alborán Sea.

|	Winter		Spring		Summer		Autumn		Annual	
	R	P-value	R	P-value	R	P-value	R	P-value	R	P-value
NW Alborán	-0.08	0.56	-0.10	0.46	0.13	0.33	-0.16	0.23	-0.17	0.0113
NC Alborán	-0.04	0.77	-0.37	0.00	-0.16	0.22	-0.50	0.00	-0.55	< 2.2e-16
NE Alborán	-0.05	0.72	-0.48	0.00	-0.35	0.01	-0.56	0.00	-0.62	< 2.2e-16
SW Alborán	-0.13	0.30	-0.57	0.00	-0.08	0.54	-0.53	0.00	-0.64	< 2.2e-16
SC Alborán	-0.30	0.02	-0.63	0.00	-0.10	0.46	-0.79	0.00	-0.74	< 2.2e-16
SE Alborán	-0.16	0.23	-0.54	0.00	-0.07	0.60	-0.75	0.00	-0.78	< 2.2e-16
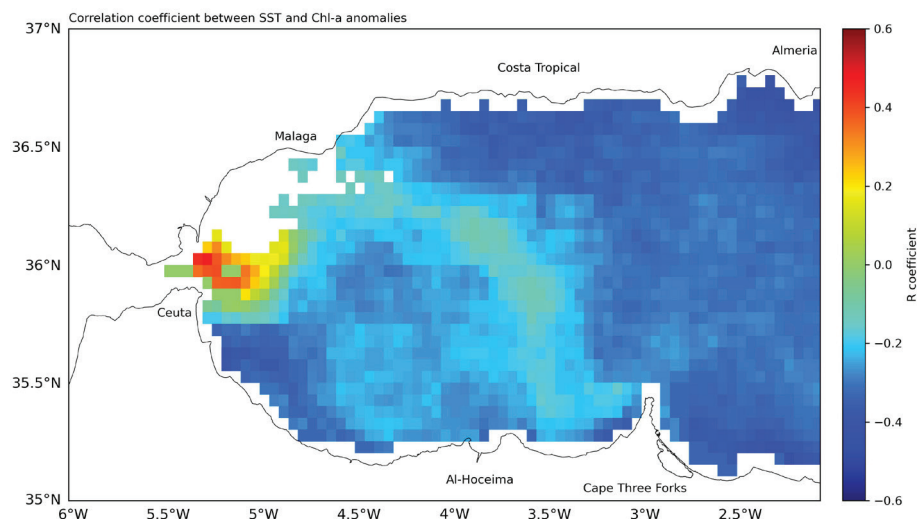
Fig. 15: Correlation coefficients pixel by pixel between monthly SST and Chl-*a* anomalies in the Alborán Sea (only statistically significant results are presented).

Alborán Sea present a highly significant negative correlation between the two parameters, varying as an annual average between - 0.6 and -0.7 (Table 3).

The exception is made for the northwestern (NW) part of the Alborán Sea near the Strait of Gibraltar as a highly hydrodynamic ecosystem. The growth of phytoplankton in this area is controlled by several mechanisms with high spatial and temporal variabilities. It depends on the nutrient load and the phytoplankton concertation, penetrating the Alborán basin, which are strongly modulated by the tidal cycles and the shear angle of AJ, allowing the offshore upwelling during the summer-autumn season (positive correlation) and intensity of westerly winds, allowing coastal upwelling in the winter season

Mediterr. Mar. Sci., 25/1, 2024, 136-150

147

(negative correlation) (Fig. 15). This clearly shows that the decrease of chlorophyll-a in Alborán Sea is strongly linked, as previously mentioned, to the warming of the sea surface water temperature. However, in the upwelling zones, it is rather the coastal areas which are more affected by these changes compared to those in the offshore areas along the Spanish coast.

In additional to this increase of sea surface temperature affecting the development of phytoplankton in Alborán Sea, the decrease of precipitations as well as river runoff for the last 20 years, up to 40% in north Africa and south Europe (Schilling *et al.*, 2012), are other factors that could enhance the decrease of chlorophyll-a in the coastal areas due the decrease of the continental organo-mineral inputs to the sea (e.g., Skliris *et al.*, 2014; Richardson & Schoeman, 2004, Hernández-Almeida *et al.*, 2011; Schroeder *et al.*, 2017; Abdellaoui *et al.*, 2017).

Conclusions

This work aimed to assess the local state of the trends of sea surface temperature (SST) and chlorophyll-a concentration (Chl-a) in the Alborán Sea in relationship to the hydrodynamic processes of the Western Alboran Gyre. The trends were estimated using the Seasonal-Trend-Loess (STL) decomposition method and Mann-Kendall test of a 20-year time series between November 2001 and December 2020. The results showed that the Alborán Sea is subject to a mean warming trend evaluated at 0.027 ± 0.008 per year and a decrease of Chl-a concentration estimated at -0.0024 ± 0.0003 µg /l per year. Summer and autumn are the most affected seasons, recording the highest positive trends of SST and highest decreasing trends of chlorophyll-a. We believe that this warming of the Alborán Sea is related to the warming of the adjacent Atlantic Ocean waters, which subsequently are transported in the Alborán Sea through the strait of Gibraltar. However, inside the basin, the impact of this warming is not uniform but shows a strong spatial variability linked to the hydrodynamic characteristics of the AJ-WAG system, which controls thermal ventilation and vertical mixing, and masks the relationship between the two water systems (Atlantic Ocean and Alborán Sea). The northern part of the basin shows a strong decrease of Chl-a concentration, probably linked to the increase of temperature of sea surface waters coming from the Atlantic, particularly areas where the upwelling phenomena is active during the summer-autumn seasons. The southern part is also subject to warming and decreasing of chlorophyll of its sea surface waters, particularly the central part off the Moroccan coast which is affected by the gyre during the summer-autumn seasons. A strong decrease of chlorophyll is also observed in coastal areas, especially on the Moroccan coast, which can be linked not only to the rise of temperature but also to the lack of precipitation and river runoff, which has become very rare these last decades.

All these changes will have a negative impact on the yields of fishery resources in the Alborán Sea with signif-icant repercussions on fishing activity (MedECC, 2020). The continuation of this work is highly recommended to understand the future evolution of the marine ecosystem in the Alborán basin as a very special gyre system and part of the western Mediterranean Sea. In particular, the effects of global warming that have become a threat to the ecological balance of local biodiversity and sustainability of marine resources. The results obtained here can represent a reference state for future studies.

References

Abdellaoui, B., Berraho, A., Falcini, F., Santoleri, J.R., Sammartino M. et *al., 2017*. Assessing the Impact of Temperature and Chlorophyll Variations on the Fluctuations of Sardine Abundance in Al-Hoceima (South Alboran Sea). *Journal of Marine Science: Research & Development,* 7 (4), 1-11.

Allain, G., Petitgas, P., Lazure, P., 2001. The influence of mesoscale ocean processes on anchovy (*Engraulis encrasicolus*) recruitment in the Bay of Biscay estimated with a three-dimensional hydrodynamic mode. *Fisheries Oceanography,* 10 (2), 151-163.

Berthon, J.-F., Zibordi, G., 2004. Bio-optical relationships for the northern Adriatic Sea. *International Journal of Remote Sensing,* 25 (7-8), 1527-1532.

Behrenfeld, M.J., O'Malley, R.T., Boss, E.S., Westberry, T.K., Graff. J.R. *et al.*, 2016. Revaluating ocean warming impacts on global phytoplankton. *Nature Climate Change,* 6 (3), 323-330.

Bryden, H.L., Stommel, H.M., 1982. Origin of the Mediterranean outflow. *Journal of Marine Research,* 40 (S), 55-71.

Cleveland, R.B., Cleveland, W.S., McRae, J.E., Terpenning, I., 1990. STL: A Seasonal-Trend Decomposition Procedure Based on Loess. *Journal of Official Statistics,* 6, 3-73.

Colella, S., Falcini, F., Rinaldi, E., Sammartino, M., Santoleri, R., 2016. "Mediterranean Ocean Color Chlorophyll Trends." *PloS one,* 11 (6), e0155756.

Criado-Aldeanueva, F., Del Río, J., García-Lafuente, J., 2008. Steric and mass-induced Mediterranean Sea level trends from 14 years of altimetry data. *Glob Planet Chang,* 60 (3-4), 563-575.

Criado-Aldeanueva, F., Soto-Navarro, J., 2020. Climatic indices over the Mediterranean Sea: A review. *Applied Sciences,* 10 (17), 5790.

D'Ortenzio, F., Marullo, S., Ragni, M., d'Alcalà, M.R., Santoleri, R., 2002. Validation of empirical SeaWiFS algorithms for chlorophyll-a retrieval in the Mediterranean Sea: A case study for oligotrophic seas. *Remote Sensing of Environment,* 82 (1), 79-94.

D'Ortenzio, F., Ribera D'Alcalá, M., 2009. On the trophic regimes of the Mediterranean Sea: a satellite analysis. *Biogeosciences,* 6 (2), 139-148.

Falcini, F., Palatella, L., Cuttitta, A., Nardelli, B.B, Lacorata, G. *et al.,* 2015. The role of hydrodynamic processes on anchovy eggs and larvae distribution in the sicily channel (Mediterranean Sea): a case study for the 2004 data set. *PloS one,* 10 (4), e0123213.

Fu, Y., Xu, S., Liu, J., 2016. Temporal-spatial variations and

148

Mediterr. Mar. Sci., 25/1, 2024, 136-150

developing trends of Chlorophyll-a in the Bohai Sea, China. *Estuarine, Coastal and Shelf Science,* 173, 49-56.

Garcia-Gorriz, E., Carr, M., 2001. Physical control of phytoplankton distributions in the Alboran Sea: A numerical and satellite approach. *Journal of Geophysical Research: Oceans,* 106 (C8), 16795-16805.

Gómez-Jakobsen, F., Mercado, J.M., Cortés, D., Ramírez, T., Salles, S. *et al.,* 2016. A new regional algorithm for estimating chlorophyll-a in the Alboran Sea (Mediterranean Sea) from MODIS-Aqua satellite imagery. *International Journal of Remote Sensing,* 37 (6), 1431-1444.

Gómez-Jakobsen, F., Ferrera, I., Yebra, L., Mercado, J.M., 2022. Two decades of satellite surface chlorophyll a concentration (1998-2019) in the Spanish Mediterranean marine waters (Western Mediterranean Sea): Trends, phenology and eutrophication assessment. *Remote Sensing Applications: Society and Environment,* 28, 100855.

González-Lanchas, A., Flores, J.A., Sierro, F.J., Bárcena, M.Á., Rigual-Hernández. *et al.,* 2020. A new perspective of the Alboran Upwelling System reconstruction during the Marine Isotope Stage 11: A high-resolution coccolithophore record. *Quaternary Science Reviews,* 245, 106520.

Giorgi, F., 2006. Climate Change Hot-Spots, *Geophysical Research Letters,* 33, L08707.

Hammond, M.L., Beaulieu, C., Henson, S.A., 2020. Regional surface chlorophyll trends and uncertainties in the global ocean. *Scientific reports,* 10 (1), 15273.

Hernández-Almeida, M.A., Bárcena, J.A., Flores, F.J., Sierro, A. Sanchez-Vidal. *et al.,* 2011. Microplankton response to environmental conditions in the Alboran Sea (Western Mediterranean): One-year sediment trap record. *Marine Micropaleontology,* 78, (1-2), 14-24.

IPCC, 2007. Pachauri, R.K and Reisinger, A. (Eds.) 2007. *Climate Change: Synthesis Report. Contribution of Working Groups I, II and III to the Fourth Assessment Report of the Intergovernmental Panel on Climate Change IPCC*, Geneva, Switzerland, 104 pp.

Kendall, M.G., 1948. Rank correlation methods. *Journal of the Institute of Actuaries,* 75 (1), 140-141.

Krauzig, N., Falco, P., Zambianchi, E., 2020. Contrasting surface warming of a marginal basin due to large-scale climatic patterns and local forcing. *Scientific Reports,* 10 (1), 17648.

Lafuente, J.G., Vargas, J.M., Criado, F., Garcia, A., Delgado, J. *et al.,* 2005. Assessing the variability of hydrographic processes influencing the life cycle of the Sicilian Channel anchovy, (*Engraulis encrasicolus)*, by satellite imagery. *Fisheries Oceanography,* 14 (1), 32-46.

Lett, C., Penven, P., Ayón, P., Freon, P., 2007. Enrichment, concentration and retention processes in relation to anchovy (*Engraulis encrasicolus*) and larvae distributions in the northern Humboldt upwelling ecosystem. *Journal of Marine Systems,* 64 (1-4), 189-200.

Lopez-Parages, J., Gomara, I., Rodríguez-Fonseca, B., García-Lafuente, J., 2022. Potential SST drivers for Chlorophyll-a variability in the Alboran Sea: A source for seasonal predictability? *Frontiers in Marine Science*, 9, 931832.

Macias, D., Garcia-Gorriz, E., Stips, A., 2013. Understanding the Causes of Recent Warming of Mediterranean Waters. How Much Could Be Attributed to Climate Change? *PloS one,* 8 (11), e81591.

Mann, H.B., 1945. Nonparametric tests against trend. *Econometrica,* 13, 245-259.

Mercado, J.M., Cortés, D., Ramírez, T., Gómez, F., 2012. Decadal weakening of the wind-induced upwelling reduces the impact of nutrient pollution in the Bay of Málaga (western Mediterranean Sea). *Hydrobiologia,* 680 (1), 91-107.

Mercado, J.M., Gómez-Jakobsen, F., 2022. Seasonal variability in phytoplankton light absorption properties: Implications for the regional parameterization of the chlorophyll a specific absorption coefficient. *Continental Shelf Research,* 232, 104614.

MedECC, 2020. Cramer, W., Guiot, J., Marini, K. (eds.) 2020*. First Mediterranean Assessment Report, Climate and Environmental Change in the Mediterranean Basin – Current Situation and Risks for the Future*. Union for the Mediterranean, Plan Bleu, UNEP/MAP, Marseille, France, 632pp.

Moradi, M., 2020. Trend analysis and variations of sea surface temperature and chlorophyll-a in the Persian Gulf. *Marine Pollution Bulletin,* 156, 111267.

Miller, K.A., Fluharty. D.L., 1992. El Niño and variability in the north-eastern Pacific Salmon fishery: implications for coping with climate change, p. 49-88. In: *Climate variability, climate change and fisheries.* Glantz, M.H. (Ed.), Cambridge University Press, Cambridge, UK.

Moyle, P.B., Cech, J.J., 2004 (5th Ed). *Fishes: An Introduction to Ichthyology*. Prentice Hall. Upper Saddle River. NJ. 612 pp.

Nykjaer, L., 2009. Mediterranean Sea surface warming 1985–2006*. Climate Research,* 39 (1), 11-17.

Palatella, L., Bignami, F., Falcini, F., Lacorata, G., Lanotte, A.S. *et al.,* 2014. Lagrangian simulations and interannual variability of anchovy egg and larva dispersal in the Sicily Channel, *Journal of Geophysical Research: Oceans,* 119 (2), 1306-1323.

Pastor, F., Valiente, J.A., Palau, J.L., 2019. Sea surface temperature in the Mediterranean: Trends and spatial patterns (1982-2016). *Pure Applied Geophysics,* 175, 4017-4029.

Perretti, C., 2015. Reducing Uncertainty in Data-Poor Assessments Using Seasonal-Trend Decomposition EFSC, *National Marine Fisheries Service, Woods Hole, MA.*

Pisano, A., Marullo, S., Artale, V., Falcini, F., Yang, C. *et al.,* 2020. New Evidence of Mediterranean Climate Change and Variability from Sea Surface Temperature Observations. *Remote Sensing,* 12, 132.

Rixen, M., Beckers, J.M., Levitus, S., Antonov, J., Boyer, T. *et al.,* 2005. The Western Mediterranean Deep Water: a proxy for climate change*. Geophysical Research Letters,* 32 (12), 1-4.

Richardson, A.J., Schoeman, D.S., 2004. Climate impact on plankton ecosystems in the Northeast Atlantic. *Science,* 305 (5690), 1609-1612.

Rykaczewski, R.R., Checkley, Jr DM., 2008. Influence of ocean winds on the pelagic ecosystem in upwelling regions. *Proceedings of the National Academy of Sciences,* 105 (6), 1965-1970.

Sabatés, A., Olivar, M.P., Salat, J., Palomera, I., Alemany, F., 2007. Physical and biological processes controlling the distribution of fish larvae in the NW Mediterranean. *Progress in Oceanography,* 74 (2-3), 355-376.

Sánchez-Garrido, J.C., Lafuente, J.G., Fanjul, E.Á., Sotillo,

M.G., Francisco, J., 2013. What does cause the collapse of the Western Alboran Gyre? Results of an operational ocean model. *Progress in Oceanography*, 116, 142-153.

Santoreli, R., Böhm, E., Schiamo, M.E., 1994. The sea surface temperature of the Western Mediterranean Sea: historical satellite thermal data. p. 155-175. In: *Seasonal and inter-annual variability of the Western Mediterranean Sea*. La Violette, P.E. (Ed.): American Geophysical Union, Washington, DC.

Santos, A.M.P., Chícharo, A., Dos Santos, A., Moita, T., Oliveira, P.B. *et al.,* 2007. Physical-biological interactions in the life history of small pelagic fish in the Western Iberia Upwelling Ecosystem. *Progress in Oceanography,* 74 (2-3), 192-209.

Sarhan, T., García-Lafuente, J., Vargas, M., Vargas, J.M, Plaza, F., 2000. Upwelling mechanisms in the northwestern Alboran Sea. *Journal of Marine Systems,* 23 (4), 317-331.

Sen, P.K., 1968. Estimates of the regression coefficient based on Kendall's tau. *Journal of the American statistical association,* 63 (324), 1379-1389.

Shaltout, M., Omstedt, A., 2014. "Recent sea surface temperature trends and future scenarios for the Mediterranean Sea". *Oceanologia,* 56 (3), 411-443.

Schroeder, K., Chiggiato, J., Josey, S.A., Borghini, M., Aracri, S. *et al.,* 2017. Rapid response to climate change in a marginal sea. *Scientific Reports,* 7 (1), 1-7.

Schilling, J., Freier, K.P., Hertig, E., Scheffran, J., 2012. Climate change, vulnerability and adaptation in North Africa with focus on Morocco. *Agriculture, Ecosystems & Environment,* 156, 12-26.

Skliris, N., Marsh, R., Josey, S.A., Good, S.A., Liu, C. *et al.,* 2014. Salinity changes in the World Ocean since 1950 in relation to changing surface freshwater fluxes. *Climate dynamics,* 43 (3), 709-736.

Skliris, N., Sofianos, S., Gkanasos, A., Mantziafou, A., Vervatis, V. *et al.,* 2012. Decadal scale variability of sea surface temperature in the Mediterranean Sea in relation to atmospheric variability. *Ocean Dynamics,* 62, 13-30.

Siokou-Frangou, I., Christaki, U., Mazzoucchi, M., Montresor, M., D'Alacia, M. R. *et al.,* 2010. Plankton in the open Mediterranean Sea: a review, *Biogeosciences,* 7 (5), 1543-1586.

Tugores, M.P., Giannoulaki, M., Iglesias, M., Bonanno, A.,

Ticina, V. *et al*., 2011. Habitat suitability modeling for sardine Sardina pilchardus in a highly diverse ecosystem: *The Mediterranean Sea. Marine Ecology Progress Series,* 443, 181-205.

Vargas-Yáñez, M., García, M.J., Salat, J., García-Martínez, M.C., Pascual, J. *et al.,* 2008. Warming trends and decadal variability in the Western Mediterranean shelf, *Gobal Planet. Change,* 63, 177-184.

Vargas-Yáñez, M., Zunino, P., Benali, A., Delpy, M., Pastre, F. *et al.,* 2010. How much is the western Mediterranean really warming and salting? *Journal of Geophysical Research: Oceans,* 115 (C04001).

Vargas-Yáñez, M., Giráldez, A., Torres, P., González, M., García-Martínez, M.C. *et al*., 2020. Variability of oceanographic and meteorological conditions in the northern Alboran Sea at seasonal, inter-annual and long-term time scales and their influence on sardine (*Sardina pilchardus Walbaum 1792*) landings. *Fisheries Oceanography,* 29 (5), 367-380.

Vargas-Yañez, M., Moya, F., Balbın, R., Santiago, R., Ballesteros, E. *et al.,* 2022. Seasonal and Long-Term Variability of the Mixed Layer Depth and its Influence on Ocean Productivity in the Spanish Gulf of Cadiz and Mediterranean Sea. *Frontiers in Marine Science,* 9, 901893.

Volpe, G., Colella, S., Forneris, V., Tronconi, C., Santoleri, R., 2012. The Mediterranean Ocean Colour Observing System – system development and product validation, *Ocean Science,* 8 (5), 869-883.

Volpe, G., Colella, S., Brando, V.E., Forneris, V., Padula, F. *et al.,* 2019. Mediterranean ocean colour Level 3 operational multi-sensor processing. *Ocean Science,* 15 (1), 127-146.

Wernand, M.R., Van der Woerd, H.J., Gieskes, WWC., 2013. Trends in Ocean Colour and Chlorophyll Concentration from 1889 to 2000, Worldwide. *PLOS one,* 8 (6), e63766.

Wirasatriya, A., Hosoda, K., Setiawan, J.D., Susanto, R.D., 2020. Variability of Diurnal Sea Surface Temperature during Short Term and High SST Event in the Western Equatorial Pacific as Revealed by Satellite Data. *Remote Sensing,* 12 (19), 3230.

Xu, Y., Rose, KA, Chai, F., Chavez, FP., Ayón, P., 2015. Does spatial variation in environmental conditions affect recruitment? A study using a 3-D model of Peruvian anchovy. *Progress in Oceanography,* 138, 417-430.